

# Optical Sources Near the Bright X-Ray Source in NGC 1073

Philip Kaaret

*Department of Physics and Astronomy, University of Iowa, Van Allen Hall, Iowa City, IA  
52242, USA*

## ABSTRACT

New HST observations show that the bright X-ray source in the face-on spiral galaxy NGC 1073 is located near a ring of recent star formation with an age of 8–16 Myr. This strengthens the association of X-ray sources in spiral galaxies emitting near or above the Eddington limit for a  $20M_{\odot}$  black hole with recent star formation events. Two candidate optical counterparts of the X-ray source are found. The X-ray to optical flux ratios of both are consistent with those of low-mass X-ray binaries and higher than most high-mass X-ray binaries, suggesting that reprocessing of X-rays contributes to the optical light. The optical magnitude and color of one candidate is consistent with that predicted for an X-ray binary with an initial donor mass of  $6 - 8 M_{\odot}$ . However, the same X-ray binary evolution model underestimates the X-ray luminosity. An X-ray source list for the field is presented which includes detections of the nucleus of NGC 1073, three quasars, and an M3e brown dwarf star with high proper motion.

*Subject headings:* black hole physics – galaxies: individual: NGC 1073 galaxies: stellar content – X-rays: galaxies – X-rays: black holes

## 1. Introduction

The discovery of bright X-ray sources in external galaxies has generated significant interest due to the possibility that they may be ‘intermediate-mass’ black holes suggested by the masses required to not violate the Eddington limit for the inferred high luminosities (Colbert & Mushotzky 1999; Makishima et al. 2000; Kaaret et al. 2001). However, there are alternative

interpretations of these so-called ‘ultraluminous X-ray sources’ (ULXs) in which the X-rays are beamed or the Eddington limit is violated and the existence of intermediate-mass black holes are not required. The luminosity function of X-ray point sources in external galaxies does not appear to have a break around the Eddington limit for ‘normal’ stellar mass black holes, i.e. with  $M < 20M_{\odot}$ , suggesting that objects above and below this limit and

members of the same population (Kilgard et al. 2002; Grimm, Gilfanov, & Sunyaev 2003). It is useful to study objects both below and above this limit to understand the properties of the full population.

The identification of counterparts of these X-ray sources at other wavelengths is important to understand the physical nature of these objects (Liu, Bregman, & Seitzer 2002; Pakull & Mirioni 2002; Kaaret et al. 2003; Zampieri et al. 2004; Liu, Bregman, & Seitzer 2004; Kaaret, Ward, & Zezas 2004). Classification of the spectral types of the companion stars should directly constrain the evolutionary history of the binary systems. Spectroscopy of companion stars might permit measurement of radial velocity curves providing direct constraints on the compact object mass. Characterization of the environments in which the X-ray sources are found should provide clues to their formation (Kaaret et al. 2004; Soria et al. 2004).

Here, we report on Hubble Space Telescope and Chandra X-Ray Observatory observations of the face-on spiral galaxy NGC 1073 (= UGC 2210). This galaxy contains an “Intermediate X-ray Object”, IXO 5, reported in the catalog of Colbert & Ptak (2002). This object has an X-ray luminosity of  $\sim 2 \times 10^{39}$  erg s $^{-1}$  which is below the Eddington luminosity for a  $20M_{\odot}$  black hole. However, it is significantly brighter than any persistent black hole X-ray binary in the Milky Way and lies at the transition between standard black hole X-ray binaries and ultraluminous X-ray sources.

NGC 1073 is a member of a tight group of galaxies containing the bright Seyfert galaxy NGC 1068 and some additional fainter companions. We adopt a distance

to NGC 1073 of 16.4 Mpc based on a radial velocity corrected for infall of the local group toward Virgo of 1147 km/s as reported in the LEDA catalog and a Hubble constant of 70 km/s/Mpc. NGC 1073 is notable because several quasars lie near the light of sight (Arp & Sulentic 1979). The presence of several objects in the field with both X-ray and optical emission permits us to obtain accurate relative astrometry of the X-ray and optical images. There are only two potential optical counterparts to the brightest X-ray source in the galaxy. We describe the observations and analysis in § 2, and discuss the results in § 3.

## 2. Observations and Analysis

### 2.1. HST observations

Observations of NGC 1073 were made using the Advanced Camera for Surveys (ACS) on the Hubble Space Telescope (HST) under GO program 10001 (PI Kaaret). Images were obtained in the broad band filters F435W (Johnson B) and F606W (Broad V) using the Wide-Field Camera (WFC). All the observations were made on 18 Nov 2003. The pointing was offset from either the X-ray source position or the galaxy nucleus in order to include two quasars known to emit both optical light and X-rays in the ACS field of view to allow us to align the X-ray and optical images. Each observation consisted of a two point line dither pattern with a pair of cosmic-ray split images obtained at each point in the pattern. The total exposure was 2160 s for the F435W image and 2240 s for the F606W image.

We used the images delivered by the standard ACS pipeline processing (OPUS

15.a and CALACS code version 4.4.1) which removes cosmic-rays, corrects for optical distortion, and dither combines the images. We aligned the F435W image to stars in the USNO B1.0 catalog (Monet et al. 2003) using the *imwcs* tool from the Smithsonian Astrophysical Observatory Telescope Data Center. Many of the stars in the USNO B1.0 catalog appear as multiple stars or clusters in the HST image. We selected 10 stars which appear as single stars in the HST image and have counterparts in the USNO B1.0 catalog. The standard deviation of the offsets of the stellar positions is  $0.37''$  which is comparable to the expected accuracy of the USNO B1.0 positions. With ten reference stars, the absolute astrometry of the corrected HST image should be better than  $0.2''$ . The F606W image was aligned to the aspect-corrected F435W image using the *IRAF* tools *geomap* and *geotran* (Tody et al. 1993).

## 2.2. Chandra observations

Observations of NGC 1073 were made using the Advanced CCD Imaging Spectrometer spectroscopy array (ACIS-S; Bautz et al. 1998) onboard the Chandra X-Ray Observatory. The ACIS-S was used in imaging mode and the source position for IXO 5 as reported by Colbert & Ptak (2002) was placed at the aimpoint. The *Chandra* observation (ObsID 4686; PI Kaaret) began on 9 Feb 2004 08:16:29 UT and had a useful exposure of 5.7 ks. The Chandra data were subjected to standard data processing and event screening (ASCDS version 7.1.1 using CALDB version 2.25). The total rate on the S3 chip was below 1.1 c/s for the entire observation

indicating that there were no strong background flares.

We constructed an image using all valid events on the S2 and S3 chips and used the *wavdetect* tool which is part of the *CIAO* version 3.1 data analysis package to search for X-ray sources. The list of detected sources with detection significance of  $3.5\sigma$  or higher is given in Table 1. The Chandra astrometry was aligned to the HST astrometry as described below. We computed an exposure map for an assumed source spectrum of a powerlaw with photon index of 1.5 absorbed by a column density of  $4.2 \times 10^{20} \text{ cm}^{-2}$  which is the total Galactic H I column density along the line of sight (Dickey & Lockman 1990). In order to give some indication of the spectral shape of each source, we calculate the the ratio of the Chandra counts in the 1–7 keV band to counts in the 0.3–7 keV band. We searched for X-ray variability by comparing the photon arrival times for each source to the distribution expected for a constant source with the same average flux using a Kolmogorov-Smirnoff (KS) test. No background subtraction was performed. Marginal evidence for variability was found for two sources: IXO 5 (source #2) which is variable at a confidence level of 94% and the quasar J024333.6+012222 (source #6) which is variable at a confidence level of 95%.

Three quasars are detected with Chandra. These are QSO B0240+011 and QSO B0241+011 which were previously detected with ROSAT (Colbert & Ptak 2002) and J024333.6+012222 (Veron-Cetty & Veron 1996). The nucleus of NGC 1073 is detected at a luminosity (assuming isotropic emission) of  $1.4 \times 10^{39} \text{ erg s}^{-1}$  in

TABLE 1  
X-RAY SOURCES NEAR NGC 1073

	S/N	Counts	RA	DEC	Error	Flux	Hardness	Comment
1	65.0	162	02 43 33.401	+01 21 37.23	0.1	$26.0 \pm 2.0$	0.45	QSO B0240+011
2	22.5	44	02 43 38.158	+01 24 11.28	0.1	$6.8 \pm 1.0$	0.73	IXO 5
3	19.1	50	02 43 39.533	+01 21 09.91	0.1	$10.6 \pm 1.5$	0.74	QSO B0241+011
4	14.6	34	02 43 37.852	+01 29 05.95	0.2	$5.6 \pm 1.0$	0.54	
5	14.3	28	02 43 40.515	+01 22 33.99	0.2	$4.3 \pm 0.8$	0.86	Nucleus
6	8.7	26	02 43 33.553	+01 22 21.90	0.3	$4.0 \pm 0.8$	0.69	J024333.6+012222
7	6.6	24	02 43 22.088	+01 28 52.70	0.1	$4.4 \pm 0.9$	0.36	LP 590-443
8	5.7	10	02 43 38.276	+01 25 36.01	0.2	$1.7 \pm 0.5$	0.54	
9	4.7	8	02 43 32.560	+01 24 06.19	0.2	$1.4 \pm 0.5$	0.89	
10	4.7	9	02 43 39.010	+01 24 39.07	0.2	$1.4 \pm 0.5$	1.00	
11	4.6	9	02 43 42.627	+01 23 15.51	0.1	$1.4 \pm 0.5$	0.33	Star
12	4.6	19	02 43 57.150	+01 18 33.95	0.4	$4.8 \pm 1.1$	0.85	
13	3.5	7	02 43 33.347	+01 22 01.89	0.2	$1.2 \pm 0.4$	0.87	Star

NOTE.—Table 1 includes for each source: the source number; S/N – the significance of the source detection as calculated by *wavdetect*; Counts - the net counts in the 0.3–7 keV band; RA and DEC – the position of the source in J2000 coordinates; Error - the statistical error on the source position in arcseconds, note that this does not include errors in the overall astrometry; Flux – the source flux in units of  $10^{-14}$  erg cm $^{-2}$  s $^{-1}$  in the 0.3–7 keV band calculated assuming a power law spectrum with photon index of 1.5 and corrected for the Galactic absorption column density of  $4.2 \times 10^{20}$  cm $^{-2}$ ; Hardness - the hardness ratio defined as the ratio of counts in the 1–7 keV band to counts in the 0.3–7 keV band. The useful exposure was 5.7 ks.

the 0.3–7 keV band. There is an X-ray source (#7) with a relatively soft spectrum within 2'' of the position of LP 590-443 which is a M3e brown dwarf star with H $\alpha$  emission and high proper motion (Cook & Reid 2000).

IXO 5 is clearly detected with a position offset by 2.9'' from that reported by Colbert & Ptak (2002). This is well within the ROSAT position uncertainty. We fit the X-ray spectrum of the source using the *XSPEC* spectral fitting tool which is part of the *LHEASOFT* X-ray data analysis package and response matrices calculated using *CIAO*. Not many photons were detected from IXO 5, so constraints on the spectral parameters are poor. An adequate fit was obtained with an absorbed power-law spectrum. The best fit parameters were photon index of  $1.3^{+0.8}_{-0.4}$  and an equivalent hydrogen absorption column density

of  $N_H = 6^{+30}_{-2} \times 10^{20}$  cm $^{-2}$ . The lower bound on  $N_H$  was fixed to the Galactic H I column density along the line of sight. The source flux from the spectral fit is consistent with that listed in Table 1.

### 2.3. Optical counterparts to X-ray sources

We overlaid the Chandra X-ray source positions on the aspect corrected F435W image. We found 6 probable matches between X-ray sources and bright optical sources within the estimated uncertainty of 0.6'' at 90% confidence of the *Chandra* aspect solution (see the Chandra aspect pages at <http://cxc.harvard.edu/cal/ASPECT/celmon>). The Chandra sources with optical counterparts are sources #1, #3, #5, #6, #11, and #13. The first two sources are the X-ray emitting quasars discussed earlier. Source #3 lies on the ACIS-S2 chip rather

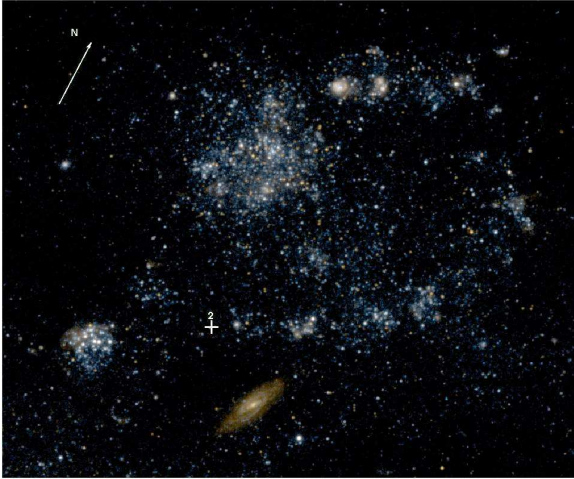


Fig. 2.— Image of the region near IXO 5. The colors are as in Fig. 1. The white cross labeled “2” shows the position of IXO 5. The white arrow points North and has a length of  $5''$ .

than the S3 chip where the bright X-ray source is located and we chose not to use it for the astrometric solution. Source #6 is the nucleus of the galaxy and is unsuitable for astrometry. We used the remaining four sources (#1, #5, #11, and #13) to align the Chandra astrometry to that of the HST image (which had previously been aligned with the USNO B1.0 catalog). We estimate that the relative alignment is accurate to better than  $0.3''$ .

An optical image of the region near IXO 5 is shown in Fig. 2. IXO 5 appears to lie near a star-forming ring. We performed photometry of the entire field shown in Fig. 2 using DAOPHOT Classic (Stetson 1987) as translated into the Interactive Data Language (IDL) by W.B. Landsman. We applied an intensity threshold somewhat above the limiting magnitude of the images in order to select only sources for which good photometry could be obtained.

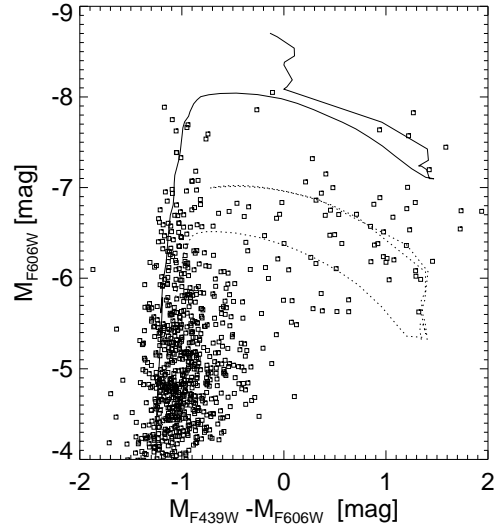


Fig. 3.— Color-magnitude diagram in  $M_{F606W}$  versus  $M_{F439W} - M_{F606W}$  for the field of Fig. 2. The magnitudes are ST magnitudes calculated for the bandpasses of the HST/WPFC2 F439W and F606W filters. The solid curve is an isochrone for an 8 Myr old stellar population from Bertelli et al. (1994) for a metallicity of  $z = 0.019$ . The dotted curve is an isochrone for a 16 Myr old stellar population.

We selected only sources for which the absolute value of the DAOPHOT peak parameter was less than 0.75 to remove extended sources and image defects and also required that the fit of the model point spread function to source intensity profile have  $\chi^2 < 3$ . These cuts remove a number of sources, including some with  $M_V \sim -10$  which are likely HII regions. However, some unresolved or marginally resolved HII regions or star clusters may remain.

To enable direct comparison with theoretical stellar isochrones, see below, we calculated ST magnitudes in the F439W and

F606W filter bandpasses of the HST Wide-Field Planetary Camera 2 (WFPC2). The reddening along the line of sight to NGC 1073 calculated from dust maps derived from COBE data (Schlegel, Finkbeiner, & Davis 1998) gives an extinction  $E(B-V) = 0.039$ . Using this extinction, a Galactic reddening law, and the *synphot* package which is part of the *STSDAS* HST data analysis software under *IRAF*, we calculated reddening corrected magnitudes from the count rates measured in the F435W and F606W filters using the spectrum of a A0V star taken from the Bruzual stellar spectrum atlas available in *synphot*. Because the WFPC2 F439W filter is well matched to the ACS/WFC F435W filter and the WFPC2 F606W filter is well matched to the ACS/WFC F606W filter, translation of the ACS/WFC count rates into ST magnitudes for the WFPC2 filter bandpasses is not strongly dependent on color. From the results presented by Sirianni et al. (2005), we estimate that the maximum error on the ST magnitudes induced by the transformation is 0.14 for  $m_{F439W}$  and 0.11 for  $m_{F606W}$ .

A color-magnitude diagram of  $M_{F606W}$  versus  $M_{F439W} - M_{F606W}$  for the field of Fig. 2 is shown in Fig. 3. The magnitudes are ST magnitudes calculated for the bandpasses of the HST/WFPC2 F439W and F606W filters. The colors are typically accurate to within  $\pm 0.4$ . There may be additional reddening within NGC 1073 or internal to the source which would affect the magnitudes and colors. Shown on the figure are isochrones for stellar populations for a metallicity of  $z = 0.019$  with ages of 8 and 16 Myr (Bertelli et al. 1994; Girardi et al. 2002).

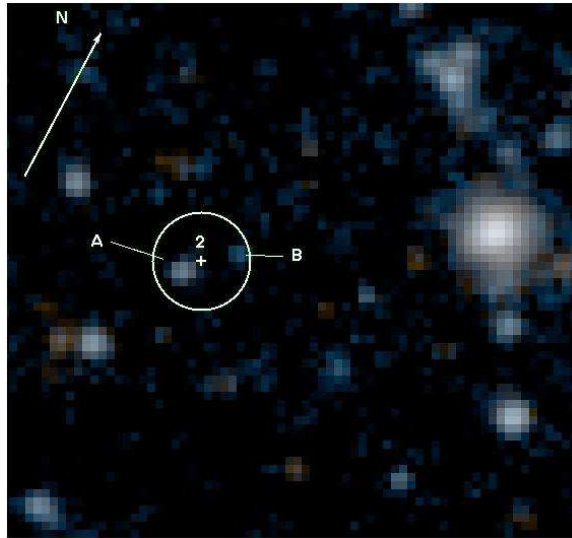


Fig. 4.— Image of the region near IXO 5. The colors are as in Fig. 1. The white cross labeled “2” shows the position of IXO 5. The white circle has a radius of  $0.3''$  and represents the relative Chandra/HST error circle. The white arrow points North and has a length of  $2''$ .

Fig. 4 shows the candidate counterparts found to IXO 5 in the F435W and F606W filters. The circle shows the relative HST/Chandra error circle with a radius of  $0.3''$ . There is one star located well within the error circle (star A) and one located near the edge (star B). Star A has a position of  $\alpha = 02^{\text{h}} 43^{\text{m}} 38^{\text{s}}.163$  and  $\delta = +01^{\circ} 24' 11''.173$  (J2000). Star B has a position of  $\alpha = 02^{\text{h}} 43^{\text{m}} 38^{\text{s}}.145$  and  $\delta = +01^{\circ} 24' 11''.438$  (J2000). Neither source appears spatially extended. The ST magnitudes of Star A uncorrected for reddening are  $25.66 \pm 0.05$  in the F435W filter and  $26.50 \pm 0.06$  in the F606W filter. For Star B, the ST magnitudes are  $26.71 \pm 0.09$  in the F435W filter and  $28.00 \pm 0.19$  in the F606W filter.

To compare the colors of the counterparts to the X-ray source with theoretical predictions, some of which are not available in HST/ACS or HST/WFPC2 bands, we calculate the equivalent B and V magnitudes. The dereddened V and B magnitudes of the two stars, calculated using the reddening correction described above and using the spectrum of an A0V star, are listed in Table 2. There may be additional reddening within NGC 1073 or internal to the source which would affect these values. Because the B-band is not a precise match to the F435W and the F606W band is significantly broader than the standard V band, the shape of the spectrum used to calculate the ACS/WFC will affect the magnitude translation. To investigate the magnitude of this effect, we recalculated the magnitudes using spectra for O5V, B5V, and A5V stars in addition to the A0V star. These stars cover a color range in  $(B - V)_0$  from  $-0.33$  to  $+0.15$ . We find that the band translation contributes an error of  $\pm 0.05$  in B and  $\pm 0.04$  in V. These band translation uncertainties have been added linearly to the photometry errors to find the total errors quoted on the magnitudes.

We also calculated dereddened ST magnitudes in the WFPC2 bands for the two candidate counterparts, see Table 2. The uncertainty due to the band conversion was calculated as in the previous paragraph. There may be additional reddening within NGC 1073 or internal to the source which would affect these values.

### 3. Discussion

IXO 5 lies near a ring of star formation shown in Fig. 2. This ring has a diame-

ter of about  $20''$  or 1.6 kpc at the distance to NGC 1073. The HII region identified by Arp, Gutiérrez, & López-Corredoira (2004) as a possible counterpart lies  $8''$  to the SE of IXO 5 and can be seen in the lower left corner of Fig. 2. This HII region is excluded as a counterpart to IXO 5, but may be part of the same star-forming event that lead to the formation of the ring. The HII region has a redshift consistent with that of NGC 1073.

A color-magnitude diagram for the objects in the ring of star formation is shown in Fig. 3. As noted above, some of the objects on the diagram may be unresolved or marginally resolved HII regions or star clusters. For comparison, we have plotted the isochrones for 8 Myr and 16 Myr old stellar populations with solar metallicity,  $z = 0.019$  and  $Y = 0.273$ , from Bertelli et al. (1994) and updated and cast into the HST/WFPC2 bands by Girardi et al. (2002). The data were obtained from the Padova web site (<http://pleiadi.pd.astro.it/>). The overall distribution of objects on the diagram is consistent with that expected for a young stellar population. The ring of star formation is similar to that found near the source X7 in NGC 4559 (Soria et al. 2004). This strengthens the idea that the bright X-ray sources found in normal spiral galaxies are associated with recent star formation events.

At a distance of 16.4 Mpc, the luminosity of IXO 5 (assuming isotropic emission) is  $2.2 \times 10^{39} \text{ erg s}^{-1}$  in the 0.3–7 keV band. This luminosity is not above the peak luminosities of stellar-mass black hole candidate X-ray transients found in the Milky Way and within the Eddington limit

TABLE 2  
OPTICAL STARS NEAR IXO 5

Magnitude	Star A	Star B
$m_{\text{F435W}}$	$25.66 \pm 0.05$	$26.71 \pm 0.09$
$m_{\text{F606W}}$	$26.50 \pm 0.06$	$28.00 \pm 0.19$
$(m_{\text{F439W}})_0$	$25.44 \pm 0.10$	$26.49 \pm 0.14$
$(m_{\text{F606W}})_0$	$26.42 \pm 0.08$	$27.92 \pm 0.21$
$(m_{\text{F439W}} - m_{\text{F606W}})_0$	$-0.98 \pm 0.18$	$-1.43 \pm 0.34$
$V$	$26.23 \pm 0.10$	$27.73 \pm 0.23$
$B - V$	$0.04 \pm 0.14$	$-0.41 \pm 0.27$
$V_0$	$26.11 \pm 0.10$	$27.61 \pm 0.23$
$M_V$	$-4.96 \pm 0.41$	$-3.46 \pm 0.46$
$(B - V)_0$	$0.00 \pm 0.14$	$-0.45 \pm 0.27$
$\xi$	$20.3 \pm 0.2$	$21.3 \pm 0.2$

NOTE.—Candidate optical counterparts to ultra-luminous X-ray source IXO 5. The first two rows give the measured quantities which are the ST magnitudes with no correction for reddening in the WFC/ACS F435W and F606W bands. The other rows give transformed magnitudes derived from the measured values. These are: the dereddened ST magnitudes in the WFPC2 F439W and F606W bands, the colors derived from these ST magnitudes, the absolute V magnitude corrected for reddening and assuming a distance of 16.4 Mpc the reddening corrected B–V color, and the X-ray to optical flux ratio, defined as  $\xi = B_0 + 2.5 \log F_X$  where  $F_X$  is the X-ray flux density at 2 keV in  $\mu\text{Jy}$  (van Paradijs & McClintock 1995).



for a ‘normal’, i.e. less than  $20M_{\odot}$ , black hole. Therefore, the system is likely an X-ray binary containing a ‘normal’ black hole rather than intermediate mass black hole. However, this luminosity is consistent with that found from the ROSAT observation made during 14-17 Jan 1998 (Colbert & Ptak 2002), which is six years before the Chandra observation. The constancy suggests that the source is persistently bright, unlike the Milky Way black hole candidate X-ray transients. The source is significantly brighter than any persistent black hole candidate X-ray binary in the Milky Way or the Magellanic Clouds, the most luminous of which is LMC X-1 at  $3 \times 10^{38} \text{ erg s}^{-1}$  (Gierlinski, Maciolek-Niedzawiecki, & Ebisawa 2001). Therefore, it appears to represent a different sort of X-ray binary, although perhaps only in evolutionary state, from those found nearby.

We found two candidate optical counterparts to IXO 5 with optical magnitudes presented in Table 2. We calculated the absolute magnitudes of the stars assuming a distance of 16.4 Mpc with an uncertainty of 20%. If the optical light comes only from the companion star, then the absolute magnitude and  $(B - V)_0$  color of the candidate counterparts can be used to classify them. Using the tables by Schmidt-Kaler in Aller (1982), we find that the possible spectral types for star A are all early supergiants, B5Ib to A8Ib. For star B, the possible spectral types are B0V-B1V, B1IV-B2IV, B2III-B3III, and B5II. This spectral classification assumes that the optical light is dominated by the companion star with little or no contribution from the accretion disk.

To help understand if reprocessed emission should be important, we calculate the X-ray to optical flux ratio, defined following van Paradijs & McClintock (1995) as  $\xi = B_0 + 2.5 \log F_X$  where  $F_X$  is the X-ray flux density at 2 keV in  $\mu\text{Jy}$ . For star A,  $\xi = 20.3$  which is higher than the X-ray to optical flux ratio for any high-mass X-ray binary within the Milky Way or Magellanic clouds except for LMC X-3. The value is consistent with that found for low-mass X-ray binaries, but somewhat lower than average. The  $(B - V)_0$  color of  $0.0 \pm 0.14$  is also consistent with those of low-mass X-ray binaries, indicating that light from an accretion disk could contribute to the optical emission. For star B, the X-ray to optical flux ratio is 21.3. This is higher than the ratios of high-mass X-ray binaries and consistent with the ratios of low-mass X-ray binaries where the accretion disk dominates over the light from the companion star. The color,  $(B - V)_0 = -0.45 \pm 0.21$ , of star B is at the blue end of the color distribution of low-mass X-ray binaries (van Paradijs & McClintock 1995). We conclude that reprocessed emission likely contributes to the optical light of either candidate. This casts doubt on the spectral classifications derived above and suggests that the effect of the X-ray emission should be taken into account to understand the optical light.

Rappaport, Podsiadlowki, & Pfahl (2005) have calculated binary evolution models for black hole X-ray binaries and made predictions concerning the optical properties including contributions from both the companion star and the accretion disk. While the applicability of such models to ultraluminous X-ray sources with higher

luminosities ( $L_X \sim 10^{40} \text{ erg s}^{-1}$ ) must remain in question because of concerns with exceeding the Eddington limit for ‘normal’ stellar-mass black holes, the models are clearly applicable to this system. Comparing the properties of the two candidate optical counterparts with those predicted for black hole X-ray binaries, i.e. Figure 12 in Rappaport, Podsiadlowki, & Pfahl (2005), we find that star B is bluer than any of the model binaries consistent with its  $M_V$ . Star A is consistent with the  $M_V$  and  $B - V$  color predicted for binaries with donor stars with original masses of  $6 - 8M_\odot$ . However, the binary evolution models appear to underestimate the X-ray luminosity. If the age of the X-ray binary is similar to the 8–16 Myr age of the star forming ring, then the predicted luminosities for binaries with original donor masses of  $6 - 8M_\odot$  are all well below  $10^{39} \text{ erg s}^{-1}$ . This may indicate some deficiency in the modeling. Binaries in this mass range may undergo mass transfer at super-Eddington rates as the donor ascends the giant branch, but this would not be expected to occur until  $\sim 100$  Myr after the formation of the binary. Also, in this case the X-ray luminosity would need to be restricted by the Eddington limit to reproduce the observed luminosity.

### Acknowledgments

PK thanks Steve Spangler and Sarah Iverson for useful discussions, the Aspen Center for Physics for its hospitality during the workshop “Compact Objects in External Galaxies”, and the referee for comments which improved the paper. PK acknowledges partial support from STScI grant HST-GO-10001.02-A and Chandra

grant CXC GO4-5086X. STSDAS and PyRAF are products of the Space Telescope Science Institute, which is operated by AURA for NASA.

### REFERENCES

- Aller, L.H. et al. 1982, Landolt-Börnstein: Numerical Data and Functional Relationships in Science and Technology, Vol. 2 Schaifers & Voigt: Astronomy and Astrophysics (Springer-Verlag, Berlin)
- Arp, H. & Sulentic, J.W. 1979, ApJ, 229, 496
- Arp, H., Gutiérrez, C.M., & López-Corredoira, M. 2004, A&A, 418, 877
- Bertelli, G., Bressan, A., Chiosi, C., Fagotto, F., & Nasi, E. 1994, A&ASS 106, 275
- Colbert, E.J.M. & Mushotzky, R.F. 1999, ApJ, 519, 89
- Colbert, E.J.M. & Ptak, A.F. 2002, ApJS, 143, 25
- Cook, J.A. & Reid, I.N. 2000, MNRAS, 318, 1206
- Dickey, J.M. & Lockman, F.J. 1990, ARA&A, 28, 215
- Girardi, L., Bertelli, G., Bressan, A., Chiosi, C., Groenewegen, M.A.T., Marigo, P., Salasnich, B., Weiss, A. 2002, A&A, 391, 195
- Gierlinski, M., Maciolek-Niedzawiecki, A., & Ebisawa, K. 2001, MNRAS, 325, 1253
- Grimm, H.-J., Gilfanov, M., Sunyaev, R. 2003, MNRAS, 339, 793

- Kaaret, P. et al. 2001, MNRAS, 321, L29
- Kaaret, P., Corbel, S., Prestwich, A.H., Zezas, A. 2003, Science, 299, 365.
- Kaaret, P., Alonso-Herrero, A., Gallagher, J.S. III, Fabbiano, G., Zezas, A., Rieke, M.J. 2004, MNRAS, 348, L28
- Kaaret, P., Ward, M.J., Zezas, A. 2004, MNRAS, 351, L83
- Kilgard, R.E., Kaaret, P., Krauss, M.I., Prestwich, A.H., Raley, M.T., Zezas, A. 2002, ApJ, 573, 138
- Liu, J.-F., Bregman, J.N., Seitzer, P. 2002, ApJ, 580, L31
- Liu, J.-F., Bregman, J.N., Seitzer, P. 2004, ApJ, 602, 249
- Makishima, K. et al. 2000, ApJ, 535, 632
- Monet, D.G. et al. 2003, AJ, 125, 984
- Ochsenbein, F., Bauer, P., Marcout, J. 2000, A&AS, 143, 221
- Pakull M.W., Mirioni L. 2002, astro-ph/0202488
- Rappaport, S.A., Podsiadlowki, Ph., Pfahl, E. 2005, MNRAS, 356, 401
- Schlegel, D., Finkbeiner, D., & Davis, M. 1998, ApJ, 500, 525
- Sirianni, M. et al. 2005, PASP, submitted
- Soria, R., Cropper, M., Pakull, M., Mushotzky, R., & Wu, K. 2004, MNRAS, to appear
- Stetson, P.B. 1987, PASJ, 99, 191
- Tody, E. 1993, in Astronomical Data Analysis Software and Systems II, A.S.P. Conference Ser., Vol. 52, eds. R.J. Hanisch, R.J.V. Brissenden, & J. Barnes, 173.
- van Paradijs, J. & McClintock J.E. in X-Ray Binaries, eds. W.H.G. Lewin, J. van Paradijs, & E.P.J. van den Heuvel, (Cambridge Univ. Press, 1995), pp. 58-125.
- Veron-Cetty, M.-P. & Veron, P. 1996, ESO Sci. Rep., 17, 1
- Zampieri, L. et al. 2004, ApJ, 603, 523

---

This 2-column preprint was prepared with the AAS L<sup>A</sup>T<sub>E</sub>X macros v5.2.

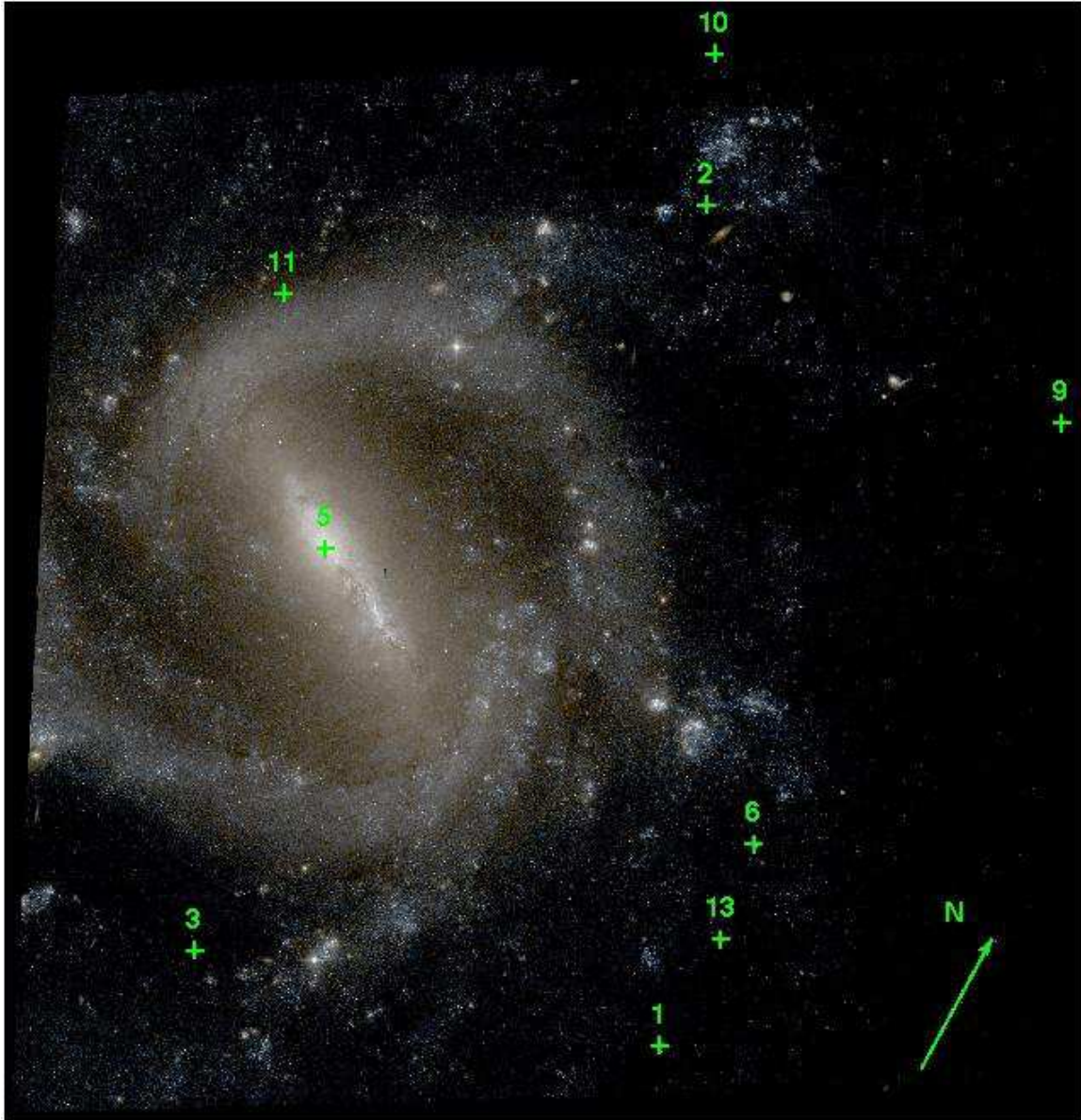


Fig. 1.— NGC 1073 imaged with the HST/ASC. Counts from the F435W filter image appear as blue; counts from the F606W filter image appear as red. A green color channel was interpolated between the F435W and F606W images to approximate true colors. The green crosses indicate the positions of Chandra sources as numbered in Table 1. Note that some of the Chandra sources lie outside the HST/ASC field of view and are not present on the image. The green arrow points North and has a length of  $10''$ .